Progress In Electromagnetics Research Letters, Vol. 87, 7–14, 2019

Dual Band Half Mode SIW Semi Circular Cavity Back Slot Antenna

Jagadeesh Dokuparthi[1, *] and Alapati Sudhakar[2]

Abstract—In this paper, a half-mode substrate integrated waveguide (HMSIW) semi-circular cavity backed antenna, using two higher order modes (TM_{210} and TM_{020}), has been proposed for dual-band operation. A semicircular slot is engraved on the top of the HMSIW structure forming a cavity that is fed by co-axial feeding to get impedance matching with the line. The theoretical operation of TM_{210} and TM_{020} modes is explained using the simulation tool. The antenna parameters such as reflection coefficient, gain, and radiation patterns have been measured for the fabricated antenna. The antenna radiates in two bands, in which the first band center frequency is 8.5 GHz, and the second band center frequency is 10.6 GHz. Peak gains at boresight direction are around 7.5 dBi and 6 dBi, respectively.

1. INTRODUCTION

Substrate integrated waveguide (SIW) technology has an advantage over conventional metallic waveguides, i.e., it has higher power handling capability and high-quality factor. The modern microwave communication systems require antenna systems with high performance and small size. To achieve this, microstrip patch antennas are frequently used to develop low profile and light weight antennas. However, these antennas have conductor losses, low power handling capability, and low efficiency [1].

A half mode SIW based semi-circular antenna with coaxial feed [2] has been designed to operate in dual-band mode in which the fundamental resonating mode is TM_{010}. A miniaturized HMSIW antenna with Grounded Co-Planar Waveguide (GCPW) feeding has been presented in [3], which resonates at a frequency of 6.78 GHz. Here, a size reduction of 50% is achieved compared with full mode SIW. A spoon-shaped slot antenna [4] is designed for circular polarization using SIW and HMSIW in which two hybrid modes are utilized and modulated to get improvement in impedance bandwidth. A compact frequency reconfigurable HMSIW antenna [5] has been designed whose resonant frequency can be varied by a varactor-loaded inter-digital capacitor. It resonates from 2.99 to 3.59 GHz by changing the bias voltage from 0 to 30 V. Transverse slots have been placed on both top and bottom surfaces of an HMSIW cavity [6] in which the wave radiates along a permanent magnetic wall. A compact S-shaped slot has been placed on the top of the HMSIW cavity in [7] to radiate at Ku-band. Two HMSIW antennas have been proposed in [8] to operate in X-band and Ka-band. Here eight slots are placed in perpendicular to the magnetic wall line, and a simple line feeding is used for each antenna. Three antennas have been proposed in [9] using FMSIW circular cavity to operate at X-band in which grounded coplanar waveguide feeding is employed. A dual-band antenna [10] has been proposed to operate at X-band and Ku-band in which an L-shaped slot is placed on the top of the cavity. One of the two arms of an L-shaped slot radiates at X-band, and the other radiates at Ku-band.

In this paper, an HMSIW semi-circular slot antenna is designed using two high-order modes for dual-band operation and fabricated on a single substrate. In Section 2, the antenna structure and dimensions are discussed. In Section 3, the design evolution and theoretical operation of the antenna are discussed, followed by its simulated and measured results in Section 4.

Received 20 June 2019, Accepted 9 August 2019, Scheduled 29 August 2019

* Corresponding author: Jagadeesh Dokuparthi (d_jagadish4@yahoo.co.in).
[1] Department of ECE, Acharya Nagarjuna University, Guntur, India. [2] Department of ECE, R.V.R & J.C College of Engineering, Guntur, India.

2. ANTENNA STRUCTURE

An HMSIW semicircular antenna with a semicircular slot is shown in Fig. 1. It is designed on an RT Duroid 5880 substrate with an overall dimension of 30 mm × 17 mm. The substrate has a dielectric constant of 2.2 and thickness $h = 1.6$ mm with a loss tangent of 0.0009. Conducting layers are placed on top and bottom of a substrate. Several metallic vias are arranged in a substrate which forms a semi-circle. The distance between the adjacent vias and diameter of each via are 1.5 mm and 1 mm, respectively, which satisfies the condition, i.e., $d/s \geq 0.5$ and $d/\lambda_0 \leq 0.1$, where d is the diameter of metal via, s the spacing between the adjacent vias, and λ_0 the free space wavelength. The radius of the semicircular cavity is 13 mm, which is denoted by 'r'. A semi-circular slot is engraved on the top conducting layer for radiation which is shown in Fig. 1(a). This slot shifts down the resonating frequencies of the cavity. This phenomenon reduces the size of the antenna. The coaxial feed and its location are optimized through parametric studies for dual-band operation. Table 1 shows the dimensions of the proposed antenna. HFSS has been used as the simulation tool.

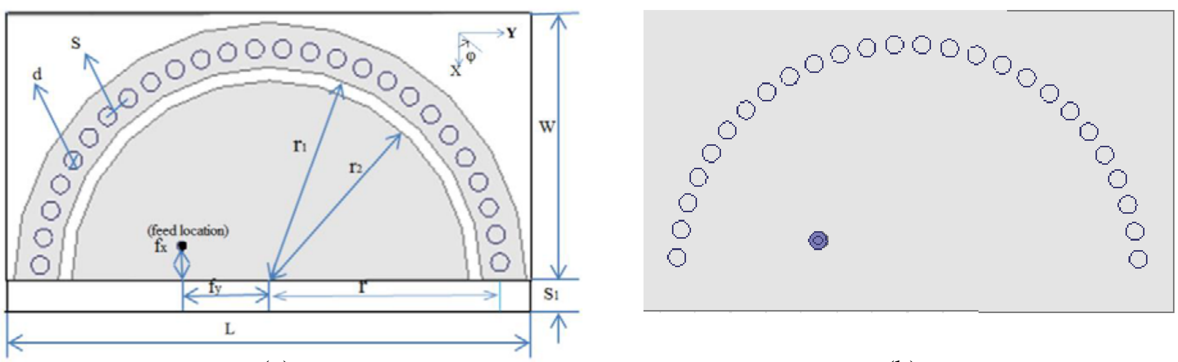

(a) (b)

Figure 1. (a) Proposed antenna structure (top view). (b) Proposed antenna structure (bottom view).

Table 1.

Parameter	L	W	S_1	r	r_1	r_2	S	d	f_x	f_y
Dimensions (mm)	30	15	2	13	12	11.25	1.5	1	2	5

3. ANTENNA ELEMENT DESIGN

Initially, a Full Mode SIW (FMSIW) circular cavity is analyzed. The resonant modes TM_{010}, TM_{110}, TM_{210}, TM_{020}, and TM_{310} are observed in HFSS simulation with resonating frequencies 6.1 GHz, 10 GHz, 13.2 GHz, 14.1 GHz, and 16.4 GHz, respectively. The expression for the resonant frequency of the FMSIW circular cavity is given in Equation (1).

$$f_{nmp} = \frac{p_{nm}c}{2\pi a\sqrt{\epsilon_r}} \tag{1}$$

where ϵ_r is the dielectric constant of the substrate, c the velocity of the light in free space, a the radius of the circular cavity, and P_{nm} the Bessel function. Here n, m, and p are the variations along the circumferential direction, radial direction, and longitudinal direction, respectively. The resonant frequencies and their E-field distributions are shown in Fig. 2 and Fig. 3, respectively.

In the next step, a ring-shaped slot is engraved on top of the FMSIW circular cavity. Here, TM_{010} mode is suppressed. Other resonant modes TM_{110}, TM_{210}, TM_{020}, and TM_{310} are shifted lower, and their resonant frequencies are 5.1 GHz, 8.6 GHz, 10.4 GHz, and 11.9 GHz, respectively. Generally, constructing slots on the cavity increase the loading effect which shifts down the resonant frequency of

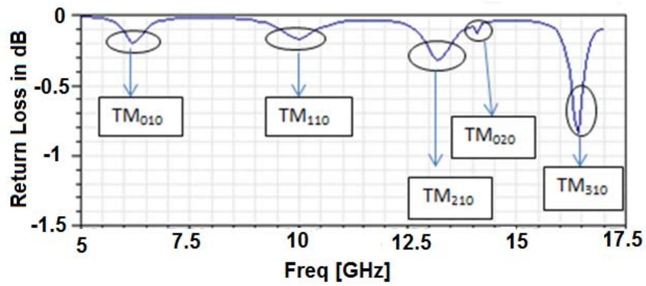

Figure 2. The simulated return loss of FMSIW cavity.

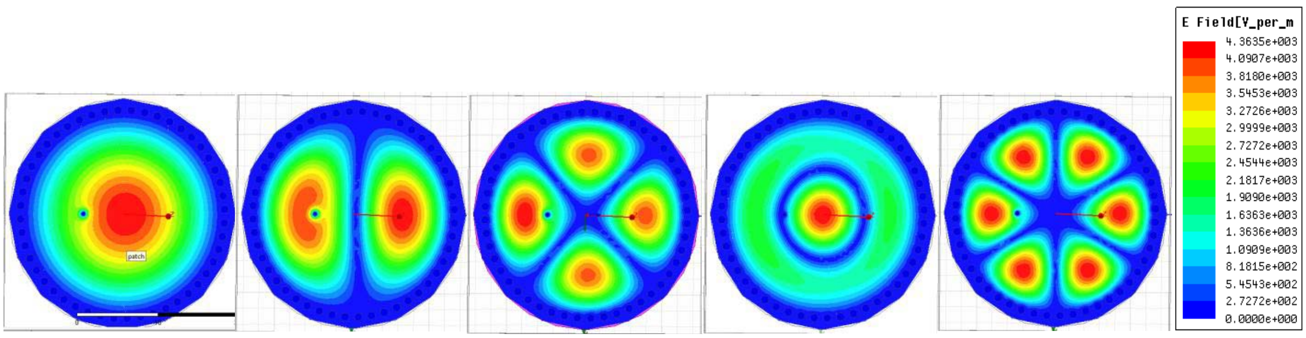

(a) (b) (c) (d) (e)

Figure 3. E-field distribution of FMSIW cavity at (a) TM_{010} Mode: 6.2 GHz. (b) TM_{110} Mode: 10 GHz. (c) TM_{210} Mode: 13.2 GHz. (d) TM_{020} Mode: 14.1 GHz. (e) TM_{310} Mode: 16.4 GHz.

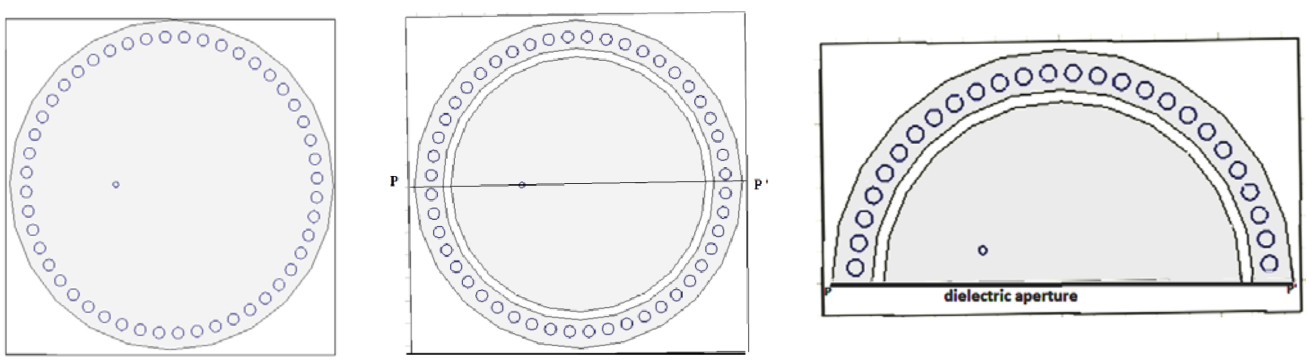

(a) (b) (c)

Figure 4. Design evolution: (a) FMSIW circular cavity. (b) FMSIW circular cavity with ring slot. (c) HMSIW cavity with slot (proposed design).

the cavity. Fig. 5 shows E-field distributions of TM_{210} and TM_{020} modes, and the line $PP^{|}$ shows a magnetic wall.

Now, the ring-shaped slot FMSIW circular cavity is divided into two parts as shown in Fig. 4. As the magnetic wall passes through feed point in FMSIW, the feed location is shifted up in HMSIW. There is a small change observed in the resonant modes of the HMSIW cavity in comparison with the ring-shaped slot FMSIW circular cavity, and it retains TM_{110}, TM_{210}, TM_{020}, and TM_{310} modes whose resonant frequencies are 5.2 GHz, 8.5 GHz, 10.6 GHz, and 11.7 GHz. Among the above four modes, impedance matching is obtained only at TM_{210} and TM_{020} modes whose E-field distributions are shown in Fig. 6.

The semi-circular slot is helpful for radiating the antenna at 8.5 GHz frequency when it is excited

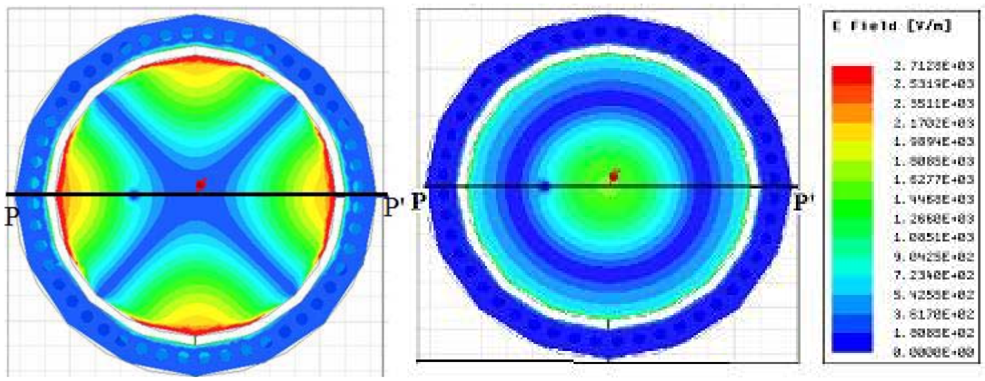

(a) (b)

Figure 5. E-field distributions of FMSIW cavity with ring slot at (a) 8.5 GHz: TM_{210}. (b) 10.6 GHz: TM_{020}.

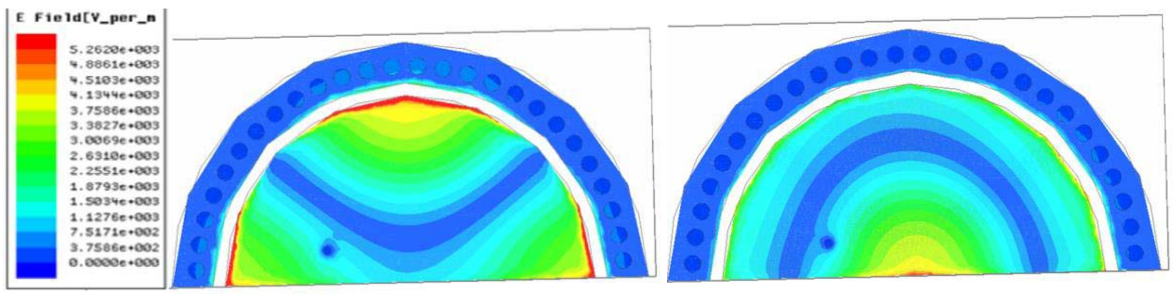

(a) (b)

Figure 6. E-field distribution of proposed design at (a) 8.5 GHz: TM_{210}. (b) 10.6 GHz: TM_{020}.

in TM_{210}. The antenna on one side is protected by vias along the semi-circular arc and on the second side is kept open along a magnetic wall (i.e., at dielectric aperture). This dielectric aperture is helpful for radiating the antenna at 10.6 GHz when it is excited in TM_{020} mode.

4. DUAL BAND HMSIW ANTENNA

An HMSIW cavity-backed antenna with a semi-circular slot is simulated in HFSS. It is observed that there are two resonant frequencies in the simulated return loss plot. Fig. 7 shows return loss vs frequency for different widths of the semi-circular slot. In Fig. 7, the resonant frequencies increase with increasing

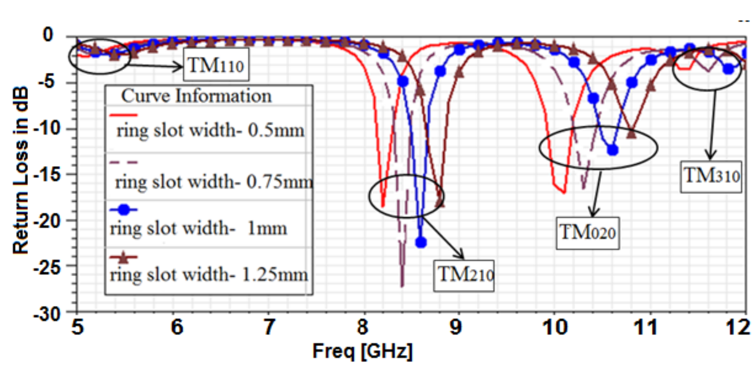

Figure 7. Simulated return loss for different slot width in HMSIW.

slot width "S_1". The equivalent capacitance of the slot is inversely proportional to the width of slot and slot resonant frequency. Finally, the resonant frequency is directly proportional to the slot width "S_1", and it is verified through simulation.

The top and bottom views of the fabricated antenna are shown in Fig. 8, and return loss is measured using Anritsu MS2037C Vector Network Analyzer. Fig. 9 shows the comparison between simulated and measured S_{11} (return loss) in dB. The measured fractional impedance bandwidths are 2.75% and 3.42% at 8.5 GHz (band1) and 10.6 GHz (band2), respectively. The measured impedance bandwidths below −10 dB are about 235 MHz and 355 MHz at band1 and band2, respectively. The center frequency deviation of 0.1 GHz is observed between the measured and simulated return losses. The simulated and measured gains are shown in the top part of Fig. 9. The simulated gain reaches up to 7.7 dBi and 6.1 dBi at the first frequency and second frequency bands, respectively. The difference between the simulated and measured gains in boresight direction is 0.1 ∼ 0.5 dBi. These deviations occur due to factors not considered for the simulations, such as fabrication errors, tolerances, and SMA connector loss.

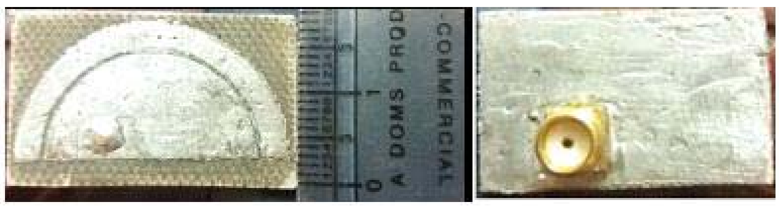

Figure 8. Fabricated antenna.

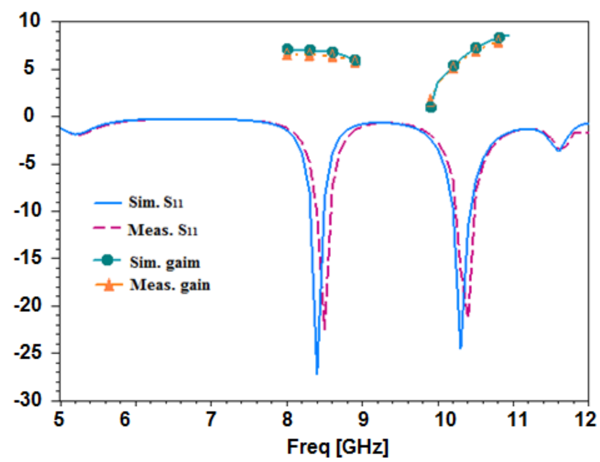

Figure 9. Return loss and gain.

As shown in Fig. 9, the antenna resonates at two frequencies: the lower one around 8.5 GHz and the higher one about 10.6 GHz. The surface current distributions at these two frequencies are shown in Fig. 10. At 8.5 GHz, most of the surface current density is situated near the semi-circular slot. At 10.6 GHz, the surface current density is high near the dielectric aperture. Thus, the radiation at the lower frequency is due to the semicircle slot, and the radiation at the higher frequency is due to the dielectric aperture.

The normalized radiation patterns at two operating bands are shown in Fig. 11. The semi-circular slot near the vias and dielectric aperture along the magnetic wall serve as a radiator coupling energy from the HMSIW cavity into free space. From Fig. 10, it is observed that the semi-circular slot affects the response at the lower operating frequency (band1) while the dielectric aperture affects the response at the higher operating frequency (band2).

E- and H-planes in the radiation pattern correspond to the y-z ($\phi = 90$) and x-z ($\phi = 0$) planes, respectively. The angular 3-dB beamwidths in E- and H-planes are about 72° and 94°, respectively.

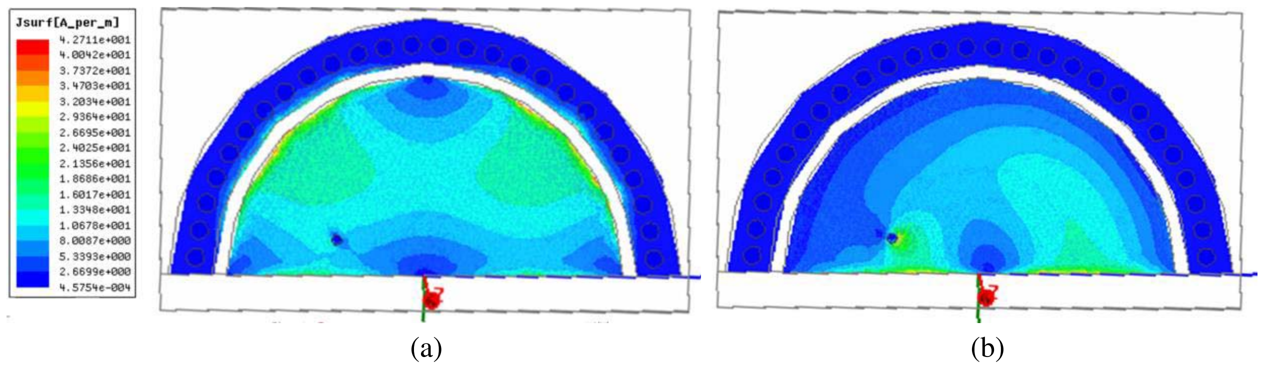

Figure 10. Surface current distribution at (a) 8.5 GHz and (b) 10.6 GHz.

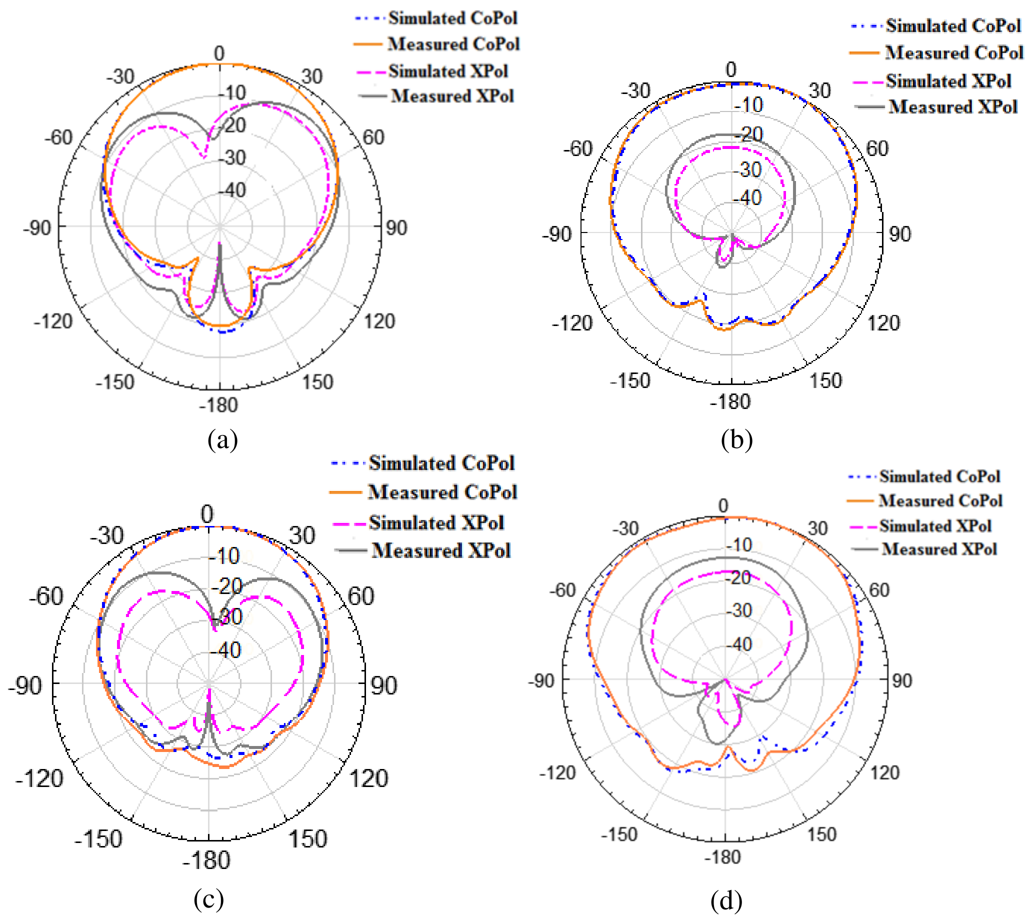

Figure 11. Simulated and measured (a) E-Plane ($\phi = 90°$) pattern at 8.5 GHz (b) H-Plane ($\phi = 0°$) pattern at 8.5 GHz (c) E-Plane ($\phi = 90°$) Patterrn at 10.6 GHz (d) H-Plane ($\phi = 0°$) pattern at 10.6 GHz.

The peak cross-polarization level (CPL) is below -15 dBi in the boresight direction, and the front-to-back-ratio (FTBR) is about 19 dBi. E- and H-planes in the radiation pattern correspond to y-z ($\phi = 90$) and x-z ($\phi = 0$) planes, respectively. The angular 3-dB beamwidths in E- and H-planes are about 108° and 71°, respectively. The peak CPL is below -16 dBi in the boresight direction, and the FTBR is about 20 dBi.

Table 2.

Ref	Frequency band (GHz)	Gain (dBi)	Fractional Impedance BW	Size
[11]	9.5 10.5	5 5	1.8% 2%	$1\lambda_l \times 0.75\lambda_l$
[12]	5 5.8	5.6 5.15	3.5% 3.1%	$1.09\lambda_l \times 0.82\lambda_l$
[13]	2.4 5.8	0.75 5.4	3.5% 3.4%	$1\lambda_l \times 1\lambda_l$
[14]	2.4 5.8	0.56 −1.59	4.9% 2.8%	$0.24\lambda_l \times 0.36\lambda_l$
[15]	12.5 14.16	5 5	0.7% 0.42%	$0.39\lambda_l \times 0.331\lambda_l$
Proposed work	8.5 10.6	7.5 6	2.75% 3.42%	$0.83\lambda_l \times 0.47\lambda_l$

λ_l is the lowest operating wavelength in free space. Table 2 shows the comparison of the proposed antenna with previously reported antennas. The size of the proposed antenna is small compared to the antennas proposed in [11–13]. Also, there is an improvement in the gain in comparison with reference antennas. However, the fractional impedance bandwidth is slightly less than reference antennas as the bandwidth of the cavity-backed antennas is directly proportional to the size of the antennas. The size of the proposed antenna is large in comparison with the antennas proposed in [14] and [15]. However, low gain and less fractional impedance bandwidth are obtained for reference antennas [14] and [15], respectively.

5. CONCLUSION

A high gain, low-profile, cavity-backed slot antenna using HMSIW is presented for dual-band operation. With proper design, TM_{210} and TM_{020} modes are excited simultaneously to operate in two bands. The antenna is a single-layered structure, and a semi-circular ring-shaped slot is placed on its top for radiation. Several antenna parameters are measured at 8.5 GHz and 10.6 GHz in which maximum gains achieved are about 7.5 dBi and 6 dBi, respectively. The antenna achieves a size reduction of approximately 50% compared to the FMSIW cavity back antenna.

REFERENCES

1. Hong, W., N. Behdad, and K. Sarabandi, "Size reduction of cavity backed slot antennas," *IEEE Trans. Antennas Propag.*, Vol. 54, No. 5, 1461–1466, May 2006.
2. Banerjee, S., S. Chatterjee, T. Mohanty, S. Ray, T. S. Sarkar, and M. Gangopadhyaya, "A compact dual-band half-mode SIW based semicircular antenna," *2016 IEEE 7th Annual Ubiquitous Computing, Electronics & Mobile Communication Conference (UEMCON)*, Oct. 20–22, 2016.
3. Kumar, A. and S. Raghavan, "A design of miniaturized half-mode SIW cavity backed antenna," *A Workshop on Advanced Antenna Technology, 2016 Indian Antenna Week (IAW 2016)*, Jun. 6–10, 2016.
4. Wu, Q., H. Wang, C. Yu, and W. Hong, "Low-profile circularly polarized cavity-backed antennas using SIW techniques," *IEEE Trans. Antennas Propag.*, Vol. 4, No. 7, 2832–2839, Jul. 2016.
5. Sam, S. and S. Lim, "Compact frequency-reconfigurable half-mode substrate-integrated waveguide antenna," *IEEE Antennas Wireless Propag Lett.*, Vol. 12, 951–954, Aug. 2013.

6. Zou, X., C.-M. Tong, H. He, and F. Geng, "Edge-radiating slot antenna based on half-mode substrate integrated waveguide," *IET Microw. Antennas Propag.*, Vol. 11, No. 8, 1106–1112, Apr. 2017.
7. Rana, B. and S. K. Parui, "Half-mode substrate integrated waveguide fed compact slot antenna," *2013 IEEE Applied Electromagnetics Conference (AEMC)*, Feb. 2015.
8. Lai, Q. H., W. Hong, Z. Q. Kuai, Y. S. Zhang, and K. Wu, "Half-mode substrate integrated waveguide transverse slot array antennas," *IEEE Trans. Antennas Propag.*, Vol. 57, No. 4, 1064–1072, Apr. 2009.
9. Dashti, H., M. Shahabadi, and M. H. Neshati, "SIW cavity-backed slot antennas with improved gain," *2013 21st Iranian Conference on Electrical Engineering*, Sept. 2013.
10. Srivastava, A., R. K. Chaudhary, A. Biswas, and M. J. Akhtar, "Dual-band L-shaped SIW slot antenna," *International Conference on Microwave and Photonics (ICMAP)*, Feb. 2014.
11. Luo, G. Q., Z. F. Hu, Y. Liang, L. Y. Yu, and L. L. Sun, "Development of low profile cavity backed crossed slot antennas for planar integration," *IEEE Antennas Propag.*, Vol. 57, 102972–102979, Oct. 2009.
12. Chaturvedi, D. and S. Raghavan,"A dual-band half-mode substrate integrated waveguide based antenna for WLAN/WBAN applications," *Int. J. RF Microw. Comput. Aided Eng.*, 2018.
13. Liu, Z. G. and Y. X. Guo, "Dual band low profile antenna for body centric communications," *IEEE Trans Antennas Propag.*, 2013.
14. Tak, J., S. Woo, J. Kwon, and J. Choi, "Dual-band dual-mode patch antenna for on/off-body WBAN communications," *IEEE Antennas Wireless Propag Lett.*, 2016.
15. Islam, M. T., N. Misran, and A. T. Mobashsher, "Compact dual band microstrip antenna for Ku-band application," *Information Technology Journal*, Vol. 9, No. 2, 354–358, 2010.